Separation and Purification Technology 134 (2014) 58–65

Contents lists available at ScienceDirect

Separation and Purification Technology

journal homepage: www.elsevier.com/locate/seppur

Pulse bubble sparging for fouling control

Sepideh Jankhah *, Pierre R. Bérubé

Department of Civil Engineering, University of British Columbia, 6250 Applied Science Lane, Vancouver, Canada

ARTICLE INFO

Article history:
Received 17 April 2014
Received in revised form 10 July 2014
Accepted 13 July 2014
Available online 21 July 2014

Keywords:
Fouling rate
Hydrodynamic conditions
Bubble size and frequency
Shear force
Power transfer efficiency
Pulse bubble sparging

ABSTRACT

The extent of fouling control in air sparged submerged membrane systems is dependent on the hydrodynamic conditions generated by sparging and the resulting shear stress induced onto membranes. Although the optimal sparging conditions (i.e. bubble size and frequency) that promote fouling control remain unclear, recent studies suggest that pulse bubble sparging is more efficient for fouling control than coarse bubble sparging. The present study demonstrated that pulse bubble sparging was substantially more effective at transferring power to the membranes than coarse bubble sparging. Pulse bubble sparging required approximately 50% less power for fouling control than coarse bubble sparging. The spatial distribution of fouling was not homogenous in the system; lower fouling rates were observed in the zone of influence of bubbles. The width of the zone of influence induced by gas sparging increased with bubble size and frequency, indicating that the size and frequency of bubbles can be optimized to minimize the required number of spargers in a system and therefore the total volume of gas required for fouling control.

1. Introduction

Fouling control through air sparging in membrane systems is governed by the hydrodynamic conditions induced under different sparging conditions (i.e. bubble size and frequency) and the resulting shear stress induced onto membranes [1,2]. However, the relationship between hydrodynamic conditions and the extent of fouling control is not well understood.

Recently, Fulton et al. [3] characterized the shear stresses that are induced onto submerged membranes by different sparging conditions. Their results indicated that the shear stresses induced on membranes are highly variable and differ substantially depending on the sparging conditions. Although the magnitude of these shear stress affect fouling control, the variation in shear stress over time has been reported to be equally if not more important for fouling control [4–7]. A number of summative parameters have been considered to relate the time variable shear stress to fouling control [8]. Of these, the extent of fouling control has been reported to be most consistently correlated to the root mean square (RMS) of time variable shear stress. However, the extent of the fouling control cannot consistently be correlated to a single summative parameter [8,9]. It is likely that other parameters, not reflected in shear stress measurements, also contribute to fouling control. In a previous study [10], the concept of power transferred to the membranes was introduced to compare the power use efficiency for different sparging conditions. Power transferred by sparged bubbles onto fibers was defined as the product of force induced onto the fibers, estimated as the product of RMS shear stress on the fibers, and the area over which the shear stress is applied in the system, and the rise velocity of the sparged bubbles. The results indicated that pulse bubble (i.e. 150–300 mL) sparging was significantly more efficient at transferring power to the membrane surface than coarse bubble sparging (0.75–2.5 mL). The results also suggested that depending on the extent of fouling control required, an optimal pulse bubble size exists.

The present study was designed to validate the use of the power transfer concept to relate the effect of gas sparging on fouling control, and to identify the sparging conditions that are optimal at achieving fouling control in terms of power use efficiency. The study considered coarse bubble sparging, as it is commonly used for fouling control in submerged hollow fiber membrane systems, and large pulse bubble sparging, as previous studies have indicated that this approach is more effective at transferring power onto membranes than coarse bubble sparging [10]. In addition recent studies have also suggested that sparging with spherical cap bubble was more effective in fouling control than coarse bubble sparging [9,11]. Some membrane manufacturers such as GE Water and Process Technologies and Evoqua have claimed that sparging with large pulse bubbles is more effective in terms of fouling control than with coarse bubbles. However, to the knowledge of the

* Corresponding author. Tel.: +1 604 822 5665.
E-mail addresses: sepidehjankhah@civil.ubc.ca (S. Jankhah), berube@civil.ubc.ca (P.R. Bérubé).

http://dx.doi.org/10.1016/j.seppur.2014.07.023
1383-5866/

Nomenclature

A	electrode area (m^2)
A_b	the area of the bubbles (m^2)
A_z	area of zone of influence of a rising bubble (m^2)
C_b	concentration of the oxidizing ion in the bulk (mole/m^3)
D	diffusion coefficient (m^2/s)
d	diameter of the probe (m)
F	Faraday constant (A s/V)
G	gravitational acceleration (9.82 m/s^2)
I	current (A)
N	number of exchanged electrons during the reaction (–)
P_{trans}	power transferred onto membranes (W)
τ_{RMS}	root mean square of shear stress (Pa)
V	volume of the bubble (m^3)
V_b	rise velocities of the bubbles (m/s)
W_z	width of zone of influence (m)
γ	shear rate (1/s)

authors, no other studies has focused on the effect of large pulse bubble sparging on the hydrodynamic conditions induced in the air sparged membrane systems and their fouling control efficiency under different sparging scenarios (i.e. bubble size and frequencies). In addition, the present study investigated the effect of sparging conditions and induced hydrodynamics on the spatial distribution of fouling in the system.

2. Material and methods

All experiments were performed in a 1 m wide, 2 m high and 15 cm thick rectangular Plexiglas system tank. A module containing seven test fibers, each 174 cm long spaced 7 cm apart was placed vertically at the center of the tank (Fig. 1). The distance between the top and the bottom bulkhead was 172 cm, enabling the 174 cm long fibers to sway.

When measuring shear stress, the module contained test fibers made of Teflon tubes with a similar diameter as that of hollow fiber membranes [12]. Shear probes were fixed half way along the height of the test fibers. Because of the symmetry of the system, shear stress was only monitored for one half of the system (i.e. four fibers) (Fig. 1b). The shear stresses induced by the sparged bubbles at the surface of the test fibers were measured using an electrodiffusion method (EDM) [12–14,2]. The reagent used for the electrochemical measurements contained 0.003 M Ferricyanide, 0.006 M Ferrocyanide, and 0.3 M potassium chloride in deoxygenated, dechlorinated tap water [3,2]. A limiting diffusion current of 550 mV was selected as described by [14]. Measurements were collected at a frequency of 200 Hz and a water temperature of 17 °C. A stainless steel anode was used in all experiments. The magnitude of shear stress was obtained from the current measured at the probes using the quasi-steady state Leveque relationship presented in Eq. (1) [15].

$$I = 0.862\, nAF c_b D^{2/3} d^{-1/3} \gamma^{1/3} \qquad (1)$$

where D is the diffusion coefficient (m^2/s), d the diameter of the probe (m), γ the shear stress (Pa), F the Faraday constant (A s/V), A the electrode area (m^2), n the number of exchanged electrons during the reaction [–], C_b the concentration of the oxidizing ion in the bulk (mole/m^3), and I is the current (A). Calibration of the probes was done ex-situ prior to all experiments as presented in [14]. Because of the turbulent nature of the hydrodynamic conditions in air-sparged membrane systems, the flow conditions at the proximity of the probes are highly transient. Therefore, the magnitude of shear calculated by the steady state solution (Eq. (1)) was corrected to account for the non-steady state conditions [2,15,16].

When filtering, the module contained hollow fiber membranes (ZW500, GE Water and Process Technologies). The fibers had a 1.8 mm diameter with a normal pore size of 0.04 mm. Each hollow fiber was connected to separate peristaltic pumps for collecting the permeate, and to the pressure transducers that measured trans-membrane pressure. The permeate flux, that was collected form 4 of the fibers (i.e. similar fiber locations as those for which shear probes were installed), was monitored over time enabling the fouling rate in each hollow fiber to be assessed. The fouling rate was quantified based on the rate of change of normalized trans-membrane pressure P_n (defined as the ratio of the trans-membrane pressure at a given time to the initial trans-membrane pressure) with respect to the volume filtered. The system average fouling rate was estimated as an average of the fouling rate of four fibers

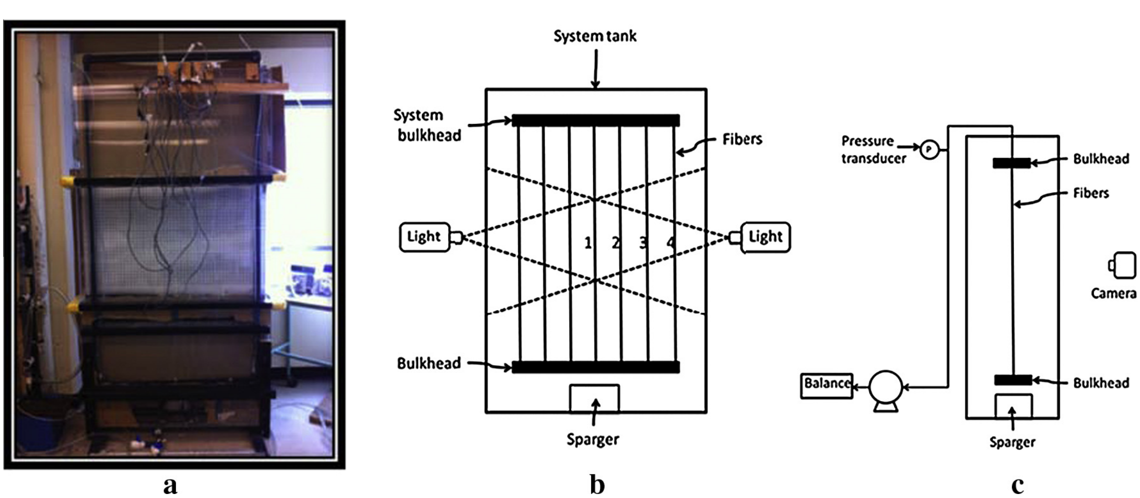

Fig. 1. Experimental system (a: picture of system; b: schematic of front view of system; probe locations identified with fiber numbers and c: schematic of side view of system).